Planetary and Space Science 121 (2016) 18–26

Contents lists available at ScienceDirect

Planetary and Space Science

journal homepage: www.elsevier.com/locate/pss

Systematic processing of Mars Express HRSC panchromatic and colour image mosaics: Image equalisation using an external brightness reference

G.G. Michael [a,*], S.H.G. Walter [a], T. Kneissl [a], W. Zuschneid [a], C. Gross [a], P.C. McGuire [a], A. Dumke [a], B. Schreiner [a], S. van Gasselt [a], K. Gwinner [b], R. Jaumann [a,b]

[a] Planetary Sciences and Remote Sensing, Department of Earth Sciences, Freie Universitaet Berlin, Malteser Strasse 74-100 Haus D, Berlin 12249, Germany
[b] Institute of Planetary Research, German Aerospace Center (DLR), Rutherfordstrasse 2, 12489 Berlin, Germany

ARTICLE INFO

Article history:
Received 10 September 2015
Accepted 1 December 2015
Available online 29 December 2015

Keywords:
Mars
Mars Express
HRSC
Mosaic
Image equalisation

ABSTRACT

After more than ten years in orbit at Mars, the coverage from the High Resolution Stereo Camera (HRSC) on the European Space Agency's Mars Express is sufficient to begin constructing mosaic products on a global scale. We describe our systematic processing procedure and, in particular, the technique used to bring images affected by atmospheric dust into visual consistency with the mosaic. We outline how the same method is used to produce a relative colour mosaic which shows local colour differences. We demonstrate the results and show that the techniques may also be applied to images from other orbital cameras.

1. Introduction

After more than ten years in orbit at Mars, the coverage from the High Resolution Stereo Camera (HRSC) on the European Space Agency's Mars Express is sufficient to begin constructing mosaic products on a global scale. HRSC is a multi-sensor pushbroom instrument comprising nine CCD line sensors to acquire multi-angle and colour images of the Martian surface (Neukum and Jaumann, 2004; Jaumann et al., 2007). The linear sensors image a line on the planet's surface perpendicular to the ground track of the spacecraft and rely on the spacecraft's orbital motion to scan the line across the surface. HRSC delivers nine superimposed image swaths, acquired at angles ranging between $\pm 18.9°$ of nadir, four of which are obtained through colour filters. Each of the CCD lines is made up of 5184 pixels, which corresponds a ground resolution of ten metres for a spacecraft altitude of 250 km. In general, the colour channel images are decreased in spatial resolution by a factor of four using on-board pixel summation to achieve lower data rates. A Super Resolution Channel (SRC) provides frame images embedded in the HRSC swath at nominally four times greater resolution.

HRSC imaging is influenced by the special characteristics of the spacecraft's orbit, which is highly elliptical with a periapsis of 330 km and an apoapsis of 10,530 km. As a consequence, there are three orbits a day and a continuous migration of the periapsis, so that the images have a continually changing illumination angle and low repetition rate. Additionally, the images' surface resolution – or inversely, their width – is strongly dependent on the spacecraft's altitude at the instant of line acquisition.

After radiometric calibration, however, the image strips still show varying brightnesses caused by differing illumination and atmospheric conditions (Fig. 1). Although there has been much work on the atmospheric correction of HRSC images (e.g. Inada et al., 2008; Hoekzema et al., 2010, 2011), the problem is highly non-trivial, and a systematically applicable procedure remains elusive. Consequently, it is not possible to derive accurate values for the absolute surface albedo from individual images. Internally, individual images do provide information on relative surface brightness, under the assumption that the atmospheric conditions are consistent along the strip. Since HRSC was conceived as a *high resolution* instrument, this limitation is not necessarily a problem: the global albedo of Mars at lower resolution is already well known, e.g. from the *Thermal Emission Spectrometer* (TES) (Christensen et al., 2001), and this can be utilised as a brightness calibration to bring the HRSC image strips to mutually consistent absolute values.

The 0.35–2.75 μm spectral response of the TES visible/near-IR bolometer (Christensen et al., 2001) is considerably broader than the HRSC panchromatic filter's 0.58–0.77 μm (Jaumann et al., 2007). We are thus implicitly assuming a correlation between the albedos in the two frequency ranges, which may not, in general, hold true. However,

* Corresponding author. Tel.: +49 30 83870584.

http://dx.doi.org/10.1016/j.pss.2015.12.002
0032-0633/

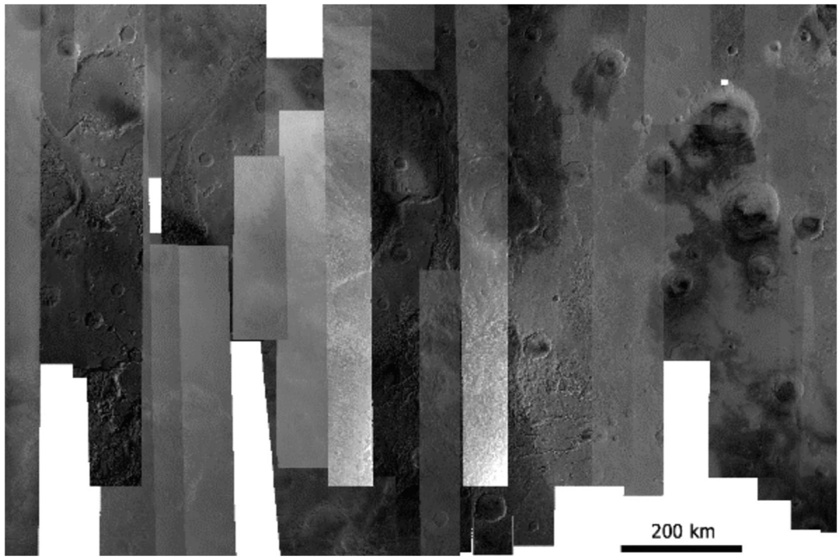

Fig. 1. After Lambert correction: strips generally have good internal illumination consistency, but atmospheric variability between strips remains strongly visible (the area shown is particularly difficult).

we emphasise that the aim of the systematic mosaic processing is to produce a set of image products which will find primary use in geological mapping projects and for the context and registration of higher resolution datasets. We hope to achieve v*isual consistency* as far as possible, making it possible to trace geomorphological features of the surface over multiple source images without the distraction of changes in brightness and contrast at the image boundaries. Absolute brightness variations in the mosaic, particularly over longer distances, need to be understood within the context of the processing methods described here.

Changes in direction of illumination cannot be corrected without loss of image quality, so these will remain: wherever possible, though, we choose to use contiguous image sequences with consistent illumination. It was a design requirement that the mosaics should be *not lower in quality* than individual image products: they are processed at the same maximum resolution as the source products (12.5 m/pix for panchromatic and 50 m/pix for colour), and the pixels can be matched back 1:1 to the sources.

In previous work, we explored other approaches to address this problem involving combinations of high-pass and low-pass filtering with smoothing (McGuire et al., 2014a, 2014b), as was done, for example, for global mosaic processing of Thermal Emission Imaging System (THEMIS) data (Edwards et al., 2011). We were unable to find an acceptable solution using only HRSC data to recover the longer range brightness variations: either the smoothing was too visible, or the remaining artefacts were too strong.

The US Geological Survey ISIS3 software suite includes a program called Equalizer, which offers both tone and contrast matching facilities. In general, it requires selected images to be designated *held* to provide a reference for the remainder. For a small group of images, where it is possible to choose a good quality image as the reference, it works perfectly. As the set of images becomes larger, and the sequences of intermediate overlapping images longer, any errors in the absolute brightness of held images propagate into the local brightness in the mosaic, appearing as striping artefacts. At a minimum, the held images need to be referenced to an external standard.

2. Preprocessing

Images are geometrically and radiometrically corrected according to the usual scheme (Jaumann et al., 2007). They are then orthorectified on a high-resolution stereo-derived digital terrain model (DTM) and map-projected for the mosaic (Gwinner et al., 2015a, 2015b). A Lambert correction is applied to equalise illumination variations resulting from the changing solar incidence angle (Walter et al., 2015) (Fig. 2).

3. Brightness adjustment

The first step is to create an intermediate resolution brightness reference map (Fig. 3). The images to be incorporated into the mosaic are divided coarsely into cells, and the mean reflectance determined for each cell. The mean value of the area corresponding to each cell is also found from the TES albedo map (Fig. 3a), and the ratio of the two gives a scaling factor to bring the image cell to an equivalent brightness. The grid of ratios representing scaling factors for the centres of the image cells is bilinearly interpolated (and extrapolated at the edges) up to the pixel dimensions of the source image. This is multiplied by the source image to produce a new image which has local average values consistent with the albedo map, while retaining relative contrasts at finer scales, consistent with the full resolution of the source image.

The cell size is chosen to be as large as possible both to avoid unnecessarily removing longer wavelength information from the source images, and to avoid reproducing finer-scale artefacts from the TES map. An important goal is to be able to obtain a close match to the brightness reference near the image edges, so that adjacent images will be consistent in average brightness. The HRSC strips are typically rather narrow in longitudinal extent, such that it is the strip width which determines the minimum cell size. We find that at least three cells across the image are needed.

Next, the brightness-scaled images are placed into a mosaic at moderate resolution (we are using 400 m/pix). The resulting mosaic appears highly consistent in brightness in a broad view (Fig. 3b), but closer inspection shows that image edges often remain visible. The edge artefacts are eliminated by applying a Gaussian blur (of 15 pixels width). The blur maintains the local average brightness while degrading the resolution. Now we have a mosaic with brightness characteristics similar to the TES albedo map, slightly higher nominal spatial resolution, but markedly reduced striping artefacts in the areas covered by HRSC and significantly higher information content (Fig. 3c).

For computational economy, we map the TES albedo range [0.0,0.35] into the 16-bit integer range [0,25,000] (leaving some

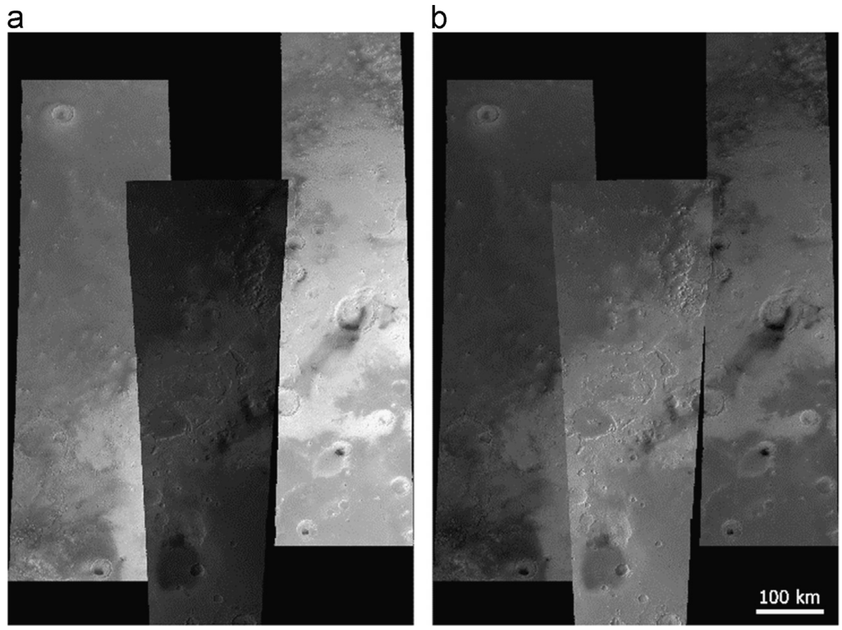

Fig. 2. Sample map-projected image strips (a) before and (b) after Lambert correction.

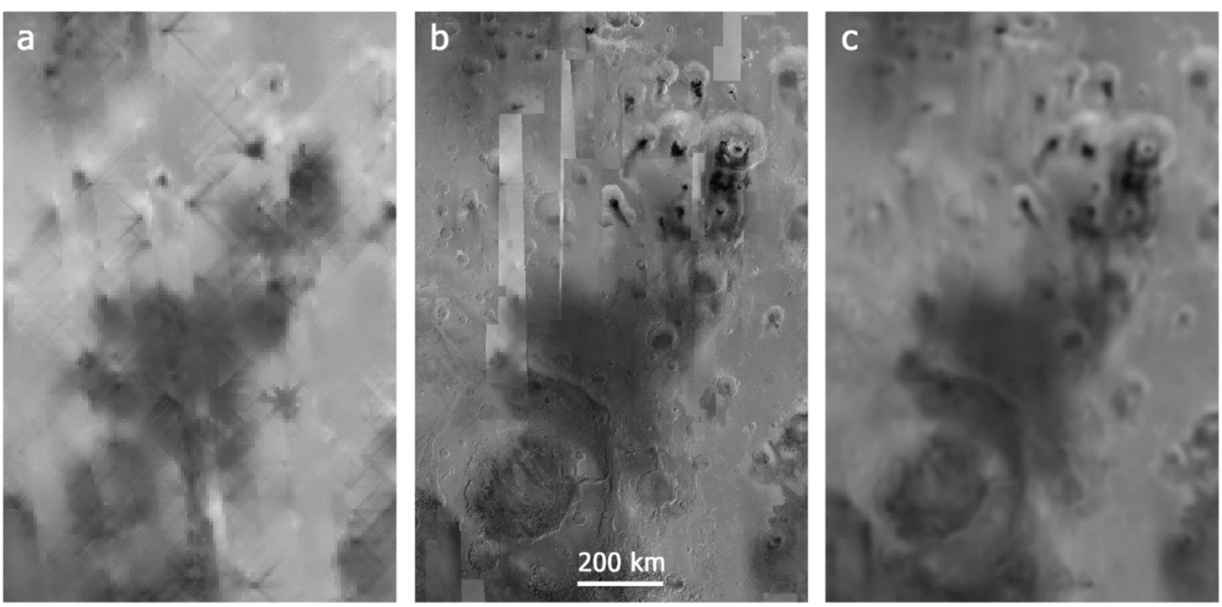

Fig. 3. Intermediate brightness reference: (a) TES, 7.5 km/pix; (b) Tied HRSC over TES, 400 m/pix; and (c) intermediate brightness reference, 3 km/pix.

overhead for brighter than average pixels), rather than carry out calculations with floating point variables.

The final step is to create a full resolution mosaic, this time using the intermediate brightness reference map as the calibration. The source images are again scaled to the reference map, but this time using smaller cells – with nine across an image strip instead of three. The higher fidelity reference map permits the use of smaller averaging cells without introducing new artefacts.

Fig. 4a shows the intermediate brightness reference mosaic before blurring: although the strip brightnesses are generally consistent, some image strip boundaries are still visible. Fig. 4b shows the same mosaic after blurring, where the boundaries are much reduced. In Fig. 4c, the final mosaic shows both consistency between image strips and the detail of the source images.

The brightness-scaled images are placed into the mosaic, feathering (i.e. fading from 0% to 100% transparency) overlapping images over a narrow range of pixels. We are using 40 pixels for a 12.5 m/pix mosaic: the optimum depends on the mosaic resolution. Note that feathering helps to hide the image boundary, but is only effective if the neighbouring image brightnesses are well matched. If they are not, the feathering softens the boundary, but *does not mask the transition.*

Additionally, feathering degrades the image quality even for a subpixel misalignment of overlapping images, so it is best to apply it over the shortest acceptable range. Occasional shared image boundaries exist where the overlap diminishes to zero along the edge (e.g. h0155_0001 with h1066_0000). In such cases, the feathering range is reduced – eventually to a hard transition.

4. Image sequencing

Images are initially placed into the mosaic in order of best ground sampling resolution, from lowest to highest. If an image overlaps existing coverage in the mosaic, the pixels of the mosaic

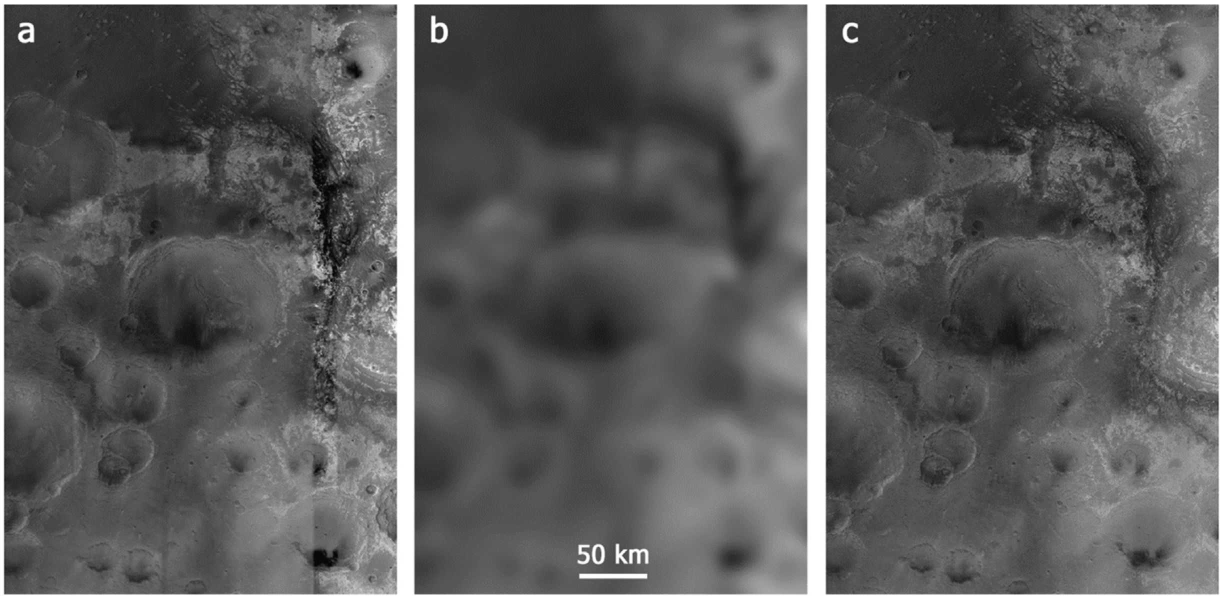

Fig. 4. (a) Brightness-scaled HRSC over TES, (b) intermediate brightness reference, and (c) final mosaic, 12.5 m/pix.

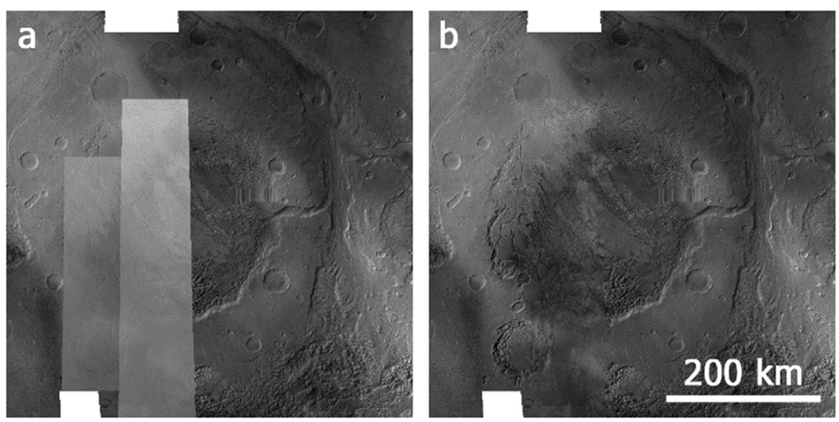

Fig. 5. (a) Mosaic with overlaid low contrast images 1903_0000 (left), 1892_0000 (centre) and (b) mosaic including images 1903_0000, 1892_0000 with contrast increases of 6 ×, 5 × (area of 1903_0000 partially covered by better image).

are replaced with those from the new image except at the image boundary, where they are feathered together.

In cases where this is not the optimal sequence, which may be for reasons of image quality or consistency of illumination, we construct a list of ordering relations. This is done by visual inspection of the assembled mosaic and comparison with individual image strips. Sequence relations are recorded in a form such as *h0103_0009* < *h1925_0000*, *h1936_0000* to indicate that *h0103_0009* should be placed below *h1925_0000* and *h1936_0000* (its east and west neighbours) or *h3180_0000* > *h2024_0001* to indicate that *h3180_0000* should lie above *h2024_0001*. This scheme allows newly acquired images to be incorporated into the processing list according to their best ground sampling distance, while maintaining sequence relations which have already been established.

The HRSC global mosaics are being compiled according to the USGS 30-quadrangle scheme, with roughly 200 HRSC image strips needed to cover a quadrangle. The sequence relations for each quadrangle are combined into a single global list so that adjacent quadrangles use identical sequencing.

5. Contrast adjustment

A significant fraction of the images show reduced contrast, a consequence of increased atmospheric scattering. Unmodified, they appear in in the processed mosaic as relatively flat bands. Their contrast can be recovered by applying a linear stretch to the histogram, although in most cases the image remains somewhat degraded in detail. The degree of stretching ranges up to values of around 6 × about the mean for images with the most atmospheric dust. The precise level is adjusted iteratively after visual inspection of the assembled mosaic (Fig. 5).

Some images show changing degrees of contrast degradation along the strip. We allow for the possibility of varying adjustment defined at multiple points: here the stretch factor is interpolated between the provided values along the image strip.

Increasing the histogram width using a multiplicative factor introduces the possibility of overflow errors: pixel values beyond the white or black points. The number of occurrences is reported during processing, allowing the factor to be reduced. Remaining overflows are clipped to the end values.

6. Colour processing

Creating a mosaic of the HRSC colour channels poses an additional challenge: not only should we be concerned with the effect of the changing atmosphere on the absolute surface brightness values, as for the nadir channel, but with its effect on the ratio between colour bands, since this is what determines the property of colour (Fig. 6).

On Earth, it is apparent that the colour of solar illumination at the surface varies over the course of a day. While at midday the light is neutral and objects are perceived to show their natural colours, towards evening the illumination colour shifts towards yellow or red as the light path through the atmosphere becomes more oblique and longer, and relatively more blue light is scattered away before reaching the surface. We expect the same effect on Mars. Additionally, the scattering efficiency is increased by the addition of fine dust particles into the atmosphere, so that we expect that the varying dust load in the Martian atmosphere may not only change the intensity of illumination at the surface, but also its colour.

We do not attempt to quantify this effect in the processing of the colour mosaic, but take a related approach to that used for the nadir channel. Instead of assuming a known brightness distribution – the TES albedo map – we begin from the known average colour of the planet, and use the HRSC colour data to elicit colour variations from that average, i.e. local changes in the colour band ratio.

This is a more restrictive starting point, but we consider the greatest value of the HRSC colour data to be in the identification of surface features at small scales which differ in their colour properties from the local environment. Such an approach allows colour features at this scale to be identified and mapped with relative ease. Further studies of their spectral properties may be made either from the source images or with locally targeted data from spectral instruments (e.g. Loizeau et al., 2010).

The processing scheme is similar to that used for the nadir mosaic processing. In the first step an intermediate brightness reference map is generated: this time, however, it is not based on a

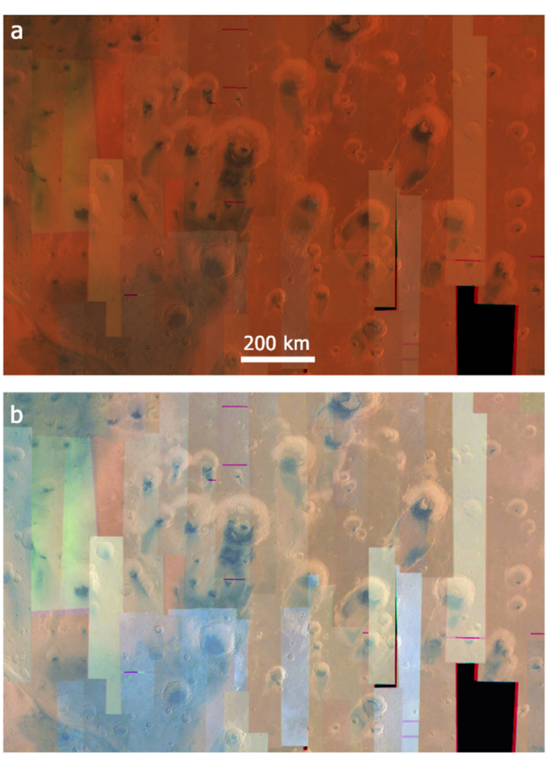

Fig. 6. Lambert corrected composite colour mosaic with (a) no additional stretch and (b) individually stretched colour channel mosaics.

lower resolution source. The cell averages are scaled to a constant value, so that the mosaic only retains local deviations from the average. The final mosaic is scaled to the intermediate brightness reference map in the same way as before.

The colour channel mosaics can be composited in various ways to produce an RGB colour mosaic. Combining the red, green, blue channels directly as an RGB image yields an average grey with locally relatively red, green or blue features showing in those colours. To produce a visually more conventional image, the channels can be combined in a fixed ratio to one another to give an average *Mars red* – the terracotta hue we expect for Mars images, with the local deviations in colour shown relative to this. Expanding the blue and green histograms relative to the red helps to bring out additional detail, since the variations in blue are much smaller. Alternative processing can be made to enhance the colour differences or to incorporate the IR channel (Jaumann et al., 2007).

Larger scale brightness features are restored by pan-sharpening the colour composite with the panchromatic mosaic (Fig. 7). The pan-sharpening is carried out by making a 16-bit RGB to HSV colour space conversion, substituting the V-channel with the panchromatic mosaic, and then converting back to RGB. This can be done either at the colour mosaic resolution of 50 m/pix or at the panchromatic resolution of 12.5 m/pix.

As the panchromatic component of the colour mosaic provides the contrast in the final product, no contrast adjustment is applied to the colour images.

The complete procedure ensures that the whole colour dataset is brought into visual homogeneity and that fine colour detail is retained as seen, for example, in the layered units in Mawrth Vallis (Fig. 7). The colour product processed this way is intended to be useful in supporting geological and geomorphological interpretations at scales close to the resolution of the HRSC instrument.

The panchromatic mosaic is distributed in its 16-bit version to maintain as much brightness detail as possible. For a colour mosaic, RGB images with 16-bit channels are more difficult to handle, as well as requiring larger files. Compressing the 16-bit range into 8 bits requires a compromise: either you choose to keep the full dynamic range, which leaves the majority of the histogram in a small subset of the 256 brightness values, or you clip the tails of the histogram so that the majority of pixels are spread over as wide a range of brightness values as possible. The former leads to a drab, low contrast image, where fine contrast differences are diminished or lost; the latter causes loss of detail in the brightest and darkest areas, e.g. highlights on crater rims or dark dune fields. A more sophisticated option is to use a Gaussian stretch, where the central parts of the histogram are mapped approximately linearly over a broad range of the output histogram, but the tails are compressed more strongly. This approach leaves good contrast in the mid-range where the majority of pixels lie and maintains detail in both the dark and bright areas. The loss of the linear relative brightness at the histogram extremes is preferable to having clipped values.

For the future, we are considering supplementing or replacing the global average Mars colour approach with a scheme identical to that used for the panchromatic mosaic. This requires equivalent global colour albedo maps corresponding to the wavelengths passed by the HRSC red, green, blue and infra-red filters, which could be derived from the Mars Express OMEGA instrument data (Bibring et al., 2004).

7. Computation

Map-projected HRSC images vary in size up to a few gigabytes, and a global mosaic at 12.5 m/pix with 16 bits/pix in simple cylindrical projection requires approximately 3 TB of storage. For convenience of processing, the mosaic is stored in tiled form – at

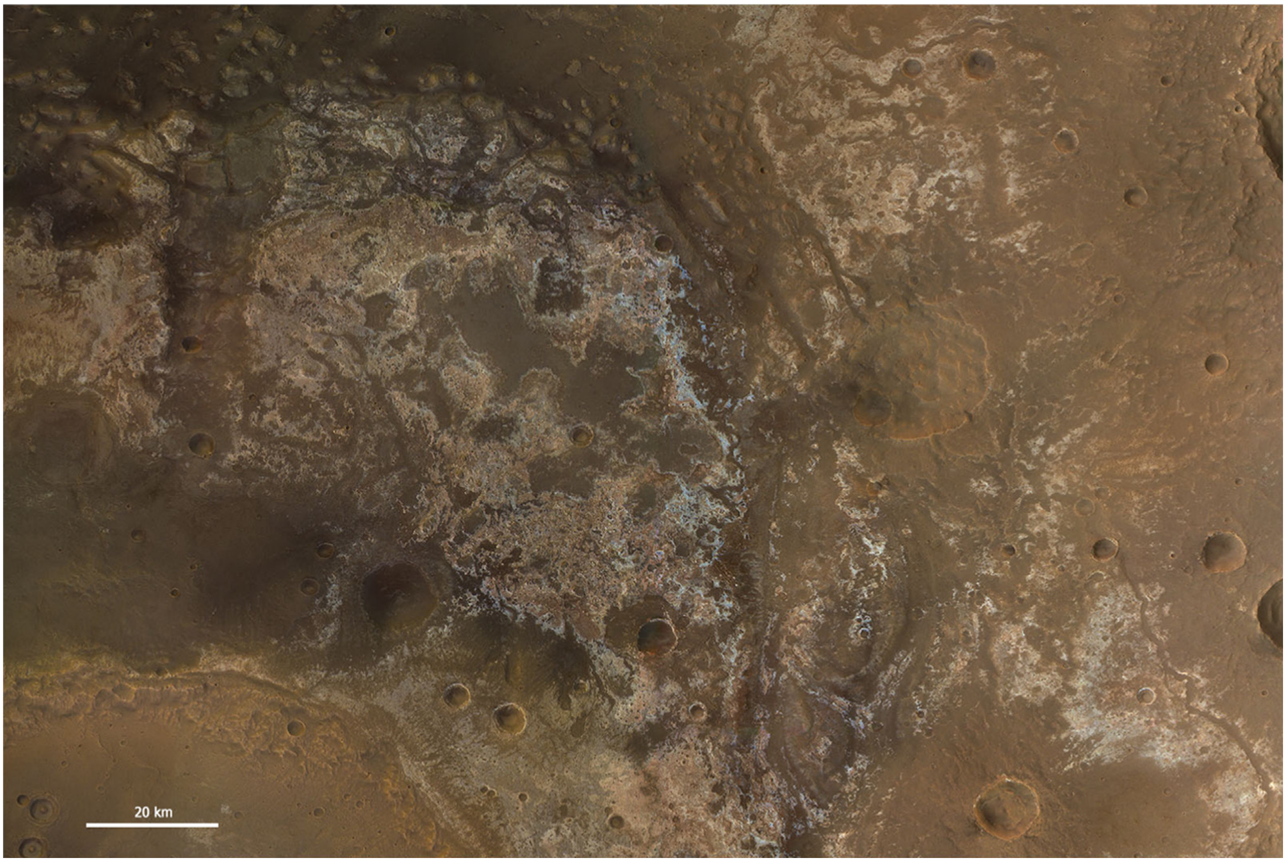

Fig. 7. Section of MC-11 showing various colour details at Mawrth Vallis: notably the exposure of a light, relatively blue, layer, and the exposures of a relatively pink layer which caps it.

present in sections of 5000 × 5000 pixels. The use of tiles makes the processing memory requirements independent of the final mosaic size.

Individual images are processed whole and then merged into the relevant mosaic tiles. On completion, the tiles may be assembled into larger regular tiles (40,000 × 40,000 gives 3 GB tiles at 16-bit), or assembled and cut into map quadrangles or sub-quadrangles. The assembled tiles are stored in GeoTIFF files with reduced-resolution image pyramids. Viewed in a GIS system the tile handling is transparent, and permits precise verification of the mosaic against the source images at pixel scale.

The current processing time for a full quadrangle nadir mosaic at 12.5 m/pix is of the order of 8 h (MC-11, 184 images, 8-core PC) using custom-written IDL software.

The manual inputs into the procedure – i.e., changes to the image sequence and individual contrast adjustments – are compiled in a GIS environment (Esri's ArcGIS) using a custom-written add-in. These are recorded in a text-file which can be appended into a universal modification list for later reprocessing of the mosaic.

7.1. *Definition of pixel grid*

There are two standards in use for defining a map-projected pixel grid. One indicates the coordinates of the centre of the upper-left pixel with a map scale to define the interval between adjacent pixels. The other indicates the coordinates of the upper-left corner of the image, i.e. the upper-left corner of the upper-left pixel, again with a map scale to define pixel spacing. Thus there is a 0.5 pixel difference between the two systems. The distinction is significant in designing a mosaic tiling system, especially when considering coregistered mosaics of differing resolutions, as the HRSC nadir, colour and DTM.

In the *pixel-centre* system, it is natural to place the first pixel on the origin (Fig. 8a). In the *pixel-edge* system, it is natural to place the first pixel edge-aligned with the origin (Fig. 8b). The divisions chosen for mosaic tiles define the tile edges: a tiled mosaic is thus a *pixel-edge* product.

For the HRSC image mosaic processing, the tiles are 5000 × 5000 pixels, and the first tile at 12.5 m/pix resolution would naturally cover the area from 0 to 62.5 km in the north and east directions from the origin. If the map-projected source images use the *pixel-centre* system, as is the case for VICAR-processed HRSC images (VICAR is an image processing system developed at JPL), it is not possible to create an origin-aligned *pixel-edge* mosaic without resampling because there is the 0.5 pixel offset between the systems. Resampling is undesirable as it degrades the image quality. The tiles can, of course, be aligned with the *pixel-centre* grid by offsetting the tile edges by 0.5 pixels. Tile edges for different resolutions, e.g. 12.5, 25 and 50 m/pix for HRSC, however, need to be offset by different amounts (6.25, 12.5 and 25 m). Thus, in this scheme, the coverage of a 25 m/pix tile will not correspond identically to the coverage of 2 × 2 12.5 m/pix tiles and the same is true for quadrangle subtiles. GIS systems will handle these differences correctly, but a user wanting to manipulate the data directly should take care to account for these small differences in tile positions.

Future projects anticipating the creation of very large mosaics may wish to consider using a *pixel-edge* aligned projection grid. Whether they retain the 100 m base figure used by HRSC with simple multiples and fractions of it (e.g. 25, 50, 75, 100, 200 m/pix), or choose a new base figure (e.g. 10 m, 1 m), the tiling boundaries will coincide at regular intervals, which simplifies data subsetting or up- or down-sampling.

8. Data gaps

Data gaps arising as a result of transmission errors or interruptions are filled by interpolation in archived data products for individual images. In constructing a mosaic, it is necessary to be able to replace missing data from an image with alternative coverage wherever possible (in Fig. 6b, nadir channel coverage gaps can be seen as black areas, and data gaps caused by some transmission loss in the green channel as horizontal magenta bars.) However, there is a trade-off to be made between data completeness and the visual homogeneity of the mosaic.

The transitions between images need to be feathered to avoid seam lines, which brings about a small amount of image degradation: where the images are misaligned, even by a fraction of a pixel, the feathering reduces the image sharpness. Differences in illumination conditions may also lead to a feathered region which is lower in quality than either of the source images. Feathering is carried out over a certain range from the image boundary: if a data gap is much smaller than this scale (we are using 15–20 pixels at 12.5 m/pix mosaic resolution), interpolation is preferable.

It was found during construction of the Viking colour mosaic that data gaps in colour bands can be restored by building a local correlation table between the missing colour and the other colour bands, and using this to reconstruct the missing values (private communication, R.L. Kirk; coding, J. Matthews). We have not yet applied the technique to HRSC, but intend to do so for future iterations of the mosaic.

9. Results

We have processed several quadrangles using orthoimages based on preliminary HRSC stereo DTMs (Scholten et al., 2005). The preliminary Oxia Palus MC-11 quadrangle panchromatic mosaic is shown in Fig. 9. It is planned that data released to the PSA and PDS archives will be based on DTM half-quadrangle mosaics for the best possible geometry (Gwinner et al., 2010, 2015b), the first of which is MC-11E. The preliminary mosaics may show small misalignments between image strips, which will be eliminated in the archival versions.

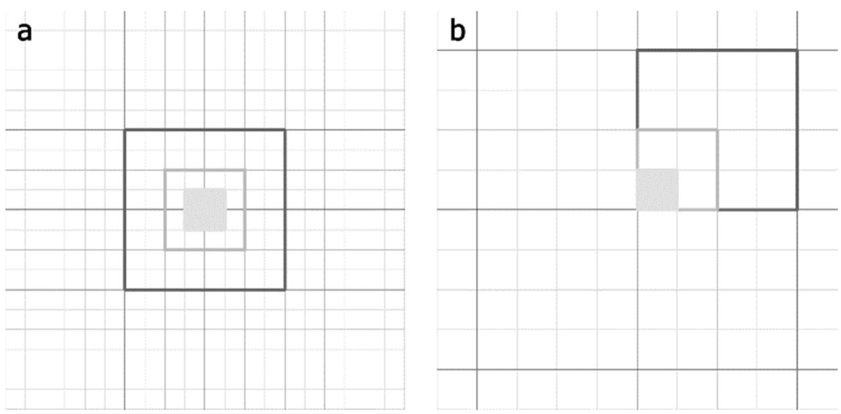

Fig. 8. Placement of pixels of dimension 12.5 m (filled squares), 25 m and 50 m (heavy outlines) in (a) pixel-centre aligned and (b) pixel-edge aligned systems.

Fig. 9. MC-11 Oxia Palus quadrangle composed from 184 image strips.

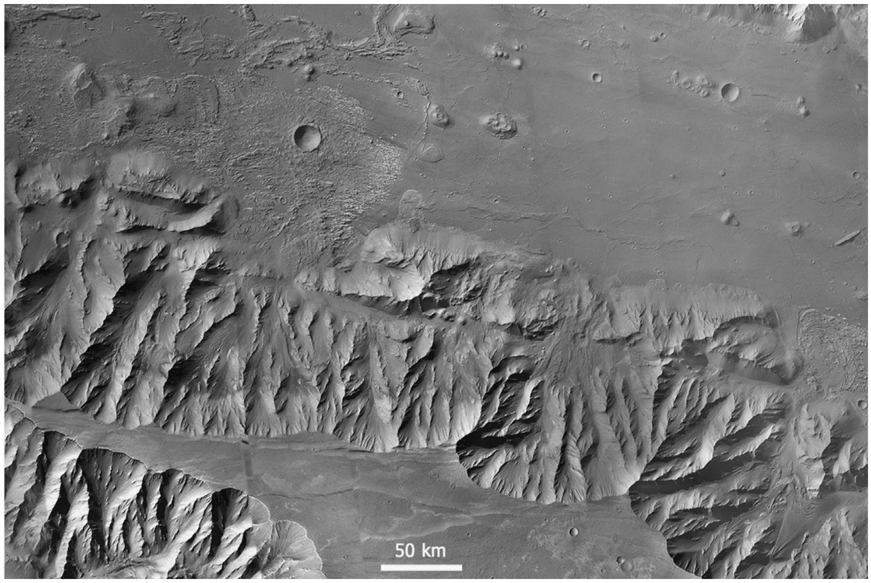

Fig. 10. Portion of CTX Coprates Chasma mosaic at 5 m/pix, made up of about ten image strips.

We have also tested the technique with images from the *Context Camera* (CTX) on *Mars Reconnaissance Orbiter* (MRO) (Malin et al., 2007), which faces similar difficulties in correcting for atmospheric effects. Fig. 10 shows a mosaic of a region of Coprates Chasma composed from about ten CTX images pre-processed in the standard way for the instrument, then put into a mosaic using TES as an external brightness reference.

10. Conclusion

We have shown that it is possible to produce visually consistent image mosaic for geological and geomorphological studies in the absence of a full correction of atmospheric effects. We have begun systematic processing of the complete HRSC dataset, working according to the US Geological Survey MC-30 quadrangle scheme. Completed quadrangles will be delivered to the ESA Planetary Science Archive (PSA) and NASA Planetary Data System (PDS) archives together with DTM mosaic products produced at the German Aerospace Center (DLR) (Gwinner et al., 2015b). The techniques can be applied to data from other imaging instruments, such as the images from the *Mars Reconnaissance Orbiter* CTX camera.

Only a limited amount of user interaction is required for image sequencing and contrast improvement, and is recorded in such a way as to guarantee a reproducible mosaicking process, and a consistent quadrangle to quadrangle and global visual appearance.

An implementation of the equalisation algorithm can be found here: http://hrscview.fu-berlin.de/software.html

Acknowledgement

We thank the two anonymous reviewers for their helpful suggestions. We also thank the HRSC experiment team at DLR Berlin and the Mars Express operations team at the European Space Operations Centre (ESOC) for their successful planning, acquisition and processing of the HRSC data. The work was supported by the German Space Agency (DLR Bonn), Grant 50QM1301 (HRSC on Mars Express), on behalf of the German Federal Ministry for Economic Affairs and Energy.

References

Bibring, J.-P., Soufflot, A., Berthé, M., Langevin, Y., Gondet, B., Drossart, P., Bouyé, M., Combes, M., Puget, P., Semery, A., Bellucci, G., Formisano, V., Moroz, V., Kottsov, V., Bonello, G., Erard, S., Forni, O., Gendrin, A., Manaud, N., Poulet, F., Poulleau, G., Encrenaz, T., Fouchet, T., Melchiori, R., Altieri, F., Ignatiev, N., Titov, D., Zasova, L., Coradini, A., Capacionni, F., Cerroni, P., Fonti, S., Mangold, N., Pinet, P., Schmitt, B., Sotin, C., Hauber, E., Hoffmann, H., Jaumann, R., Keller, U., Arvidson, R., Mustard, J., Forget, F., 2004. OMEGA: Observatoire pour la Minéralogie, l'Eau, les Glaces et l'Activité. In: Wilson, A., Chicarro, A. (Eds.), Mars Express Scientific Payload, vol. 1240. ESA Special Publication, pp. 37–49.

Christensen, P.R., Bandfield, J.L., Hamilton, V.E., Ruff, S.W., Kieffer, H.H., Titus, T.N., Malin, M.C., Morris, R.V., Lane, M.D., Clark, R.L., Jakosky, B.M., Mellon, M.T., Pearl, J.C., Conrath, B.J., Smith, M.D., Clancy, R.T., Kuzmin, R.O., Roush, T., Mehall, G.L., Gorelick, N., Bender, K., Murray, K., Dason, S., Greene, E., Silverman, S., Greenfield, M., 2001. Mars Global Surveyor Thermal Emission Spectrometer experiment: investigation description and surface science results. J. Geophys. Res. 106, 23823–23872.

Edwards, C.S., Nowicki, K.J., Christensen, P.R., Hill, J., Gorelick, N., Murray, K., 2011. Mosaicking of global planetary image datasets: 1. Techniques and data processing for Thermal Emission Imaging System (THEMIS) multi-spectral data. J. Geophys. Res. (Planets) 116, 10008.

Gwinner, K., Hauber, E., Jaumann, R., Michael, G., Hoffmann, H., Heipke, C., 2015a. Global topography of Mars from High Resolution Stereo Camera (HRSC) multi-orbit data products: the first quadrangle (MC-11E) and the landing site areas of ExoMars. In: EGU General Assembly Conference Abstracts, p. 13158.

Gwinner, K., Jaumann, R., Hauber, E., Hoffmann, H., Heipke, C., Oberst, J., Neukum, G., Ansan, V., Bostelmann, J., Dumke, A., Elgner, S., Erkeling, G., Fueten, F., Hiesinger, H., Hoekzema, N.M., Kersten, E., Loizeau, D., Matz, K.-D., McGuire, P.C., Mertens, V., Michael, G.G., Pasewaldt, A., Pinet, P., Preusker, F., Reiss, D., Roatsch, T., Schmidt, R., Scholten, F., Spiegel, M., Stesky, R., Tirsch, D., Gasselt, S., van, Walter, S., Wählisch, M., Willner, K., 2015. The High Resolution Stereo Camera (HRSC) of Mars Express and its approach to science analysis and mapping for mars and its satellites. Planet. Space Sci.

Gwinner, K., Scholten, F., Preusker, F., Elgner, S., Roatsch, T., Spiegel, M., Schmidt, R., Oberst, J., Jaumann, R., Heipke, C., 2010. Topography of Mars from global mapping by HRSC high-resolution digital terrain models and orthoimages: characteristics and performance. Earth Planet. Sci. Lett. 294, 506–519.

Hoekzema, N.M., Garcia-Comas, M., Stenzel, O.J., Grieger, B., Markiewicz, W.J., Gwinner, K., Keller, H.U., 2010. Optical depth and its scale-height in Valles Marineris from HRSC stereo images. Earth Planet. Sci. Lett. 294, 534–540.

Hoekzema, N.M., Garcia-Comas, M., Stenzel, O.J., Petrova, E.V., Thomas, N., Markiewicz, W.J., Gwinner, K., Keller, H.U., Delamere, W.A., 2011. Retrieving optical depth from shadows in orbiter images of Mars. Icarus 214, 447–461.

Inada, A., Garcia-Comas, M., Altieri, F., Gwinner, K., Poulet, F., Bellucci, G., Keller, H.U., Markiewicz, W.J., Richardson, M.I., Hoekzema, N., Neukum, G., Bibring, J.-P., 2008. Dust haze in Valles Marineris observed by HRSC and OMEGA on board Mars Express. J. Geophys. Res. (Planets) 113, 2004.

Jaumann, R., Neukum, G., Behnke, T., Duxbury, T.C., Eichentopf, K., Flohrer, J., Gasselt, S. v, Giese, B., Gwinner, K., Hauber, E., Hoffmann, H., Hoffmeister, A., Köhler, U., Matz, K.-D., McCord, T.B., Mertens, V., Oberst, J., Pischel, R., Reiss, D., Ress, E., Roatsch, T., Saiger, P., Scholten, F., Schwarz, G., Stephan, K., Wählisch, M., HRSC Co-Investigator Team, the, 2007. The high-resolution stereo camera (HRSC) experiment on Mars Express: instrument aspects and experiment conduct from interplanetary cruise through the nominal mission. Planet. Space Sci. 55, 928–952.

Loizeau, D., Mangold, N., Poulet, F., Ansan, V., Hauber, E., Bibring, J.-P., Gondet, B., Langevin, Y., Masson, P., Neukum, G., 2010. Stratigraphy in the Mawrth Vallis region through OMEGA, HRSC color imagery and DTM. Icarus 205, 396–418.

Malin, M.C., Bell, J.F., Cantor, B.A., Caplinger, M.A., Calvin, W.M., Clancy, R.T., Edgett, K.S., Edwards, L., Haberle, R.M., James, P.B., Lee, S.W., Ravine, M.A., Thomas, P.C., Wolff, M.J., 2007. Context camera investigation on board the Mars Reconnaissance Orbiter. J. Geophys. Res. (Planets) 112, E05S04.

McGuire, P.C., Walter, S.H.G., Gasselt, S., van, Dumke, A., Dunker, T., Gross, C., Michael, G., Wendt, L., Audouard, J., Ody, A., Poulet, F., 2014a. Global HRSC image mosaics of Mars: dodging for high-pass filtering, combined with low-pass-filtered OMEGA mosaics. LPI Contributions 1791, 1118.

McGuire, P.C., Walter, S.H.G., Gasselt, S. van Dumke, A., Gross, C., Michael, G., Wendt, L., 2014b. Towards automated global color mosaicking of HRSC images of Mars. In: Proceedings of the Lunar Planetary Science Conference, Lunar Planetary Institute Technical Report, p. 1899.

Neukum, G., Jaumann, R., 2004. HRSC: the High Resolution Stereo Camera of Mars Express. In: Wilson, A., Chicarro, A. (Eds.), Mars Express Scientific Payload, vol. 1240. ESA Special Publication, pp. 17–35.

Scholten, F., Gwinner, K., Roatsch, T., Matz, K.-D., Wählisch, M., Giese, B., Oberst, J., Jaumann, R., Neukum, G., 2005. Mars express HRSC data processing – methods and operational aspects. Photogramm. Eng. Remote Sens. 71, 1143–1152.

Walter, S.H.G., Michael, G., Gasselt, S.V., Kneissl, T., 2015. Photometric Lambert correction for global mosaicking of HRSC image data. In: Proceedings of the Lunar Planetary Science Conference, Lunar Planetary Institute Technical Report, p. 1434.